



Augmentation of Natural Convection Heat Transfer from a Fin by Lateral Hexagonal Perforations

Abdullah H. AlEssa^{1*} and Isam H. E. Qasem¹

¹Al-Balqa Applied University, Al-Husn University College, Al-Husn, Irbid, Jordan.

Authors' contributions

This work was carried out in collaboration between both authors. Both authors read and approved the final manuscript.

Article Information

DOI: 10.9734/BJAST/2016/12863

Editor(s):

(1) Grzegorz Golanski, Institute of Materials Engineering, Czestochowa University of Technology, Poland.

Reviewers:

(1) Pedro Dinis Gaspar, University of Beira Interior, Portugal.

(2) Mohammad Reza Safaei, University of Malaya, Malaysia.

(3) Salem Banooni, Shahid Chamran University of Ahvaz, Iran.

Complete Peer review History: <http://www.sciencedomain.org/review-history/16366>

Original Research Article

Received 22nd July 2014
Accepted 28th August 2016
Published 28th September 2016

ABSTRACT

In this study the enhancement of heat transfer from a horizontal rectangular fin subjected to natural convection provided with lateral hexagonal perforations is investigated using one dimensional finite element technique. The orientation of these perforations is described as they have two sides parallel to the base and tip of the fin. The perforated fin is compared with its equivalent solid one. The parameters considered are geometrical dimensions and thermal properties of the fin and these of the perforations. This study involves enhanced heat transfer surfaces that provide increased turbulence and a better flow distribution. Also, it considered the gain in fin area and of heat transfer coefficients due to perforations. From this study and for certain values of hexagonal dimension and spaces between perforations, it is found that there is an augmentation in heat transfer dissipation of the perforated fin over than that of the equivalent solid one. Moreover, the heat transfer enhancement of the perforated fin increases as the thickness and thermal conductivity of the fin are increased.

Keywords: Finite element; perforated fin; lateral hexagonal perforation; heat dissipation; heat transfer augmentation; natural convection.

*Corresponding author: E-mail: abdd104@yahoo.com;

NOMENCLATURES

A	: Cross sectional area of the solid fin m^2
A_c	: Cross sectional area of the lateral hexagonal perforation m^2
A_e	: Cross sectional area of the element which is perpendicular to the x axe m^2
Bi	: Biot number
b	: Lateral hexagonal perforation dimension m
h	: Overall heat transfer coefficient by natural convection for the fin surface $W/m^2 \cdot ^\circ C$
k	: Thermal conductivity of the fin material $W/m \cdot ^\circ C$
L	: Fin length m
l	: Unit vector
L_c	: Characteristic length m
Le	: Fin length m
N_e	: Number of finite element of the whole symmetry part of the perforated fin
N_f	: Number of finite element of straight parts of the symmetry part of the perforated fin (regions A and D)
N_n	: Number of finite element nodes of the whole symmetry part of the perforated fin
N_t	: Number of finite element of tapered straight parts of the symmetry part of the perforated fin (regions B and C)
N_x	: Number of perforations in x direction
N_y	: Number of perforations in y direction
Nu	: Average Nusselt number under natural convection for the fin surface
Nu_c	: Average Nusselt number of the inner lining perforation surface
OA	: Open area of the perforated surface of the perforated fin
Ra	: Rayleigh number of the fin surface
Ra_c	: Rayleigh number of the perforation inner lining surface
ROA	: Ratio of open area
OA_{max}	: Maximum open area of the perforated surface of the perforated fin
RQF	: Ratio of heat transfer dissipation rate of perforated fin to that of non-perforated one
RWF	: Ratio of the perforated fin weight to that of the non-perforated one.
S	: Distance between perforation (Perforation spacing) m
T	: Temperature $^\circ C$
t	: Fin thickness m
Ve	: Volume of the finite element m^3
W	: Fin width m

SUBSCRIPTS AND SUPERSSCRIPTS

b	: Base of the fin
e	: Finite Element
l	: Lower surface of the fin
max	: maximum
pc	: Perforation inner surface (within the perforation)
pf	: Perforated fin
ps	: Remaining solid portion of the perforated fin
sf	: Solid fin (non-perforated one)
ss	: Solid surface
s	: Side
t	: Fin tip
u	: Upper surface of fin
x	: Longitudinal direction or coordinate
y	: Lateral (Transverse) direction with the fin width or coordinate
z	: Lateral (Transverse) direction with the fin thickness or coordinate
∞	: Ambient

1. INTRODUCTION

The quick heat removal from heated surfaces and devices is very important and it becomes an important duty in the design of thermal applications. Developments of thermal systems as heat exchangers require efficient techniques to remove large amounts of heat between extended surfaces and the ambient fluid. Understanding the heat transfer and flow mechanisms provides the necessary knowledge that may leads to maximum thermal performance of high efficiency heat exchangers. In typical applications of air to fluid heat exchangers, the dominant resistance is on the air-side [1]. Therefore, improving the heat transfer on the air-side heat transfer is required by the growing demand of high efficiency heat transfer systems. Enhanced heat transfer surfaces can be designed through a combination of factors that include:- 1- Increasing fluid flow turbulence. 2- Generating secondary fluid flow patterns. 3- Reducing the thermal boundary layer thickness and 4- Increasing the heat transfer surface area [1].

The studies of augmentation or enhancement of heat transfer aims and seeks to increase heat transfer performance. The heat transfer augmentation is very important subject in heat exchangers and other thermal applications. There are many techniques which are available for augmentation of heat transfer under natural or forced convection. Those techniques may be passive methods which require no direct application of external power or active methods which require external power. The methods of heat transfer augmentation can be classified into three types, based on whether the enhancement is caused by either the heat transfer surface (surface methods), or the working fluid (fluid methods), or a combination of the two (combined methods). Surface methods include any techniques which directly involve the heat exchange surface. The primary mechanisms for thinning the boundary layer are increased free stream velocity and turbulent mixing. Secondary recirculation flows can further enhance the convective heat transfer. Flows from the core to the wall reduce the thickness of the boundary layer in the wash of the flow, and secondary flows from the wall to the core promote mixing. Flow separation and reattachment within the flow channel also contribute to heat transfer enhancement [2]. The augmentation of heat transfer can be achieved by increasing one or more of the following: 1- The heat transfer

coefficients, 2- The heat transfer surface areas [3,4]. In most cases, the area of heat transfer is increased by utilizing extended surfaces (fins) [5]. Fins as heat transfer enhancement devices have been widely in used. As the fins knowledge continues to develop, new designs come out including fins made of porous media, interrupted and perforated plates [2,3,4,5]. As the lightweight, compact, and economical fins are preferable then the optimization of the fin size is of great importance. So, the fins should be designed and fabricated in a manner that can produce a maximum heat removal with minimum fin material consumption. However, the ease of manufacturing of the fin shape should be taken into account [2,6]. Large number of studies has been conducted on optimizing fin shapes. Other studies have introduced shape modifications by cutting some material from fins to make cavities, holes, slots, grooves, or channels through the fin body to increase the heat transfer surface area, to increase the heat transfer coefficient or to increase the both [2,3 and 6]. The rough surfaces can be used to increase heat transfer as one type of the popular heat transfer augmentation techniques. The surface roughness aims at promoting surface turbulence that is intended mainly to increase the heat transfer coefficient rather than the surface area [2,3]. For the free convection from machined or formed rough surfaces with air it concluded that increases in heat transfer coefficient up to 100% [2]. The interrupted and perforated fins attributing the improvement to the restarting of the thermal boundary layer after each interruption indicating that the increase in convection coefficient is even more than enough to offsets lost area, if any [3]. Perforated plates and fins represent an example of surface interruption and are widely used in different heat exchanger, film cooling, and solar collector applications [2,3,7]. The heat transfer augmentation and friction loss performances of plate-perforated rectangular fin surfaces in a conductive-convective heat transfer system are studied. The effects of the fins having different perforation geometries on the heat exchanger performance are determined, and performance comparison of the plate-perforated fin heat exchangers relative to a reference exchanger having plate-non perforated fin surfaces is included. It is found that under certain circumstances the perforation will produce substantial improvement in heat transfer without introducing pronounced form drag. The slotted fins are seen to be the high-performance extended surfaces. Raaid R. Jassem [8] investigates experimentally the improvements of

extended surfaces by perforations. He studied enhancement of the heat transfer by natural convection in a rectangular perforated fin plates. The results show that the triangular perforation gives best values of heat transfer coefficient and then the circular, square, hexagonal, and non-perforation, respectively. R. B. Gurav et al. [9] examine heat transfer augmentation from a fin embedded with elliptical perforation under natural convection compared to the equivalent solid fin. The parameters considered were geometrical dimensions and thermal properties of the fin and that of the perforations. This study shows that the heat dissipation from the perforated fin results in improved heat transfer over the equivalent solid fin. Rupali V. et al. [10], examine the heat transfer augmentation from horizontal rectangular fins with circular perforations under natural convection compared with solid fins. The study showed that as perforations increases heat transfer rate also increases. Heat transfer enhancement of the perforated fin increases with increase in fin thickness.

This study aims mainly at examining the extent of heat transfer enhancement from a horizontal rectangular fin under natural convection as a result of introducing surface modification to the fin. The modification in this work is a lateral vertical equilateral hexagonal perforation made through the fin body in the direction of its thickness (in z direction). The study investigates the effects of perforations on heat transfer dissipation rate of the fin. Furthermore, the performance of the modified perforated fin is compared to the corresponding solid (non-perforated) fin. In particular, the study eventually attempts to make the best use of the material and size of a given fin, which involves some sort of optimization (maximization).

2. ASSUMPTIONS FOR ANALYSIS

Generally the classical treatment of fins assumes one-dimensional heat conduction. This is valid when the Biot number is very small (i.e, $Bi < 0.01$) [11,12]. The perforated fin with hexagonal perforations which is considered in this study is shown in Fig. 1. In this fin, the conduction heat transfer is dominant in x direction. However, the values of (Bi_y) and (Bi_z) are less than 0.01, then the heat transfer in (y) and (z) directions can be assumed lumped and one dimensional heat transfer solution can be considered. Fig. 2 shows the symmetry part considered for heat transfer analysis (shown hatched). For this part the

transverse Biot number in or along the y-axis (Bi_y) can be calculated as:

$$Bi_y = \frac{h_{ps} \left(S_y + b \left(0.5 + \sin \left(\frac{\pi}{6} \right) \right) \right)}{K} \quad (1)$$

And the Biot number in or along the z-axis (Bi_z) can be calculated as:

$$Bi_z = \frac{h_{ps} \cdot t}{2K} \quad (2)$$

If the values of (Bi_y) and (Bi_z) greater than 0.01 then the heat transfer solution must be in two or three dimensions. According to the above Biot numbers which are a constraints for the one dimensional solution discussion, then the forgoing analysis is based on the following assumptions:

1. Steady state and one-dimensional heat conduction.
2. Homogeneous fin material with constant thermal conductivity.
3. Uniform base and ambient temperatures.
4. Uniform heat transfer coefficient overall the whole fin solid surface (perforated or solid).
5. Uniform heat transfer coefficient within the perforation.

3. HEAT TRANSFER ANALYSIS

According to the previous assumptions, the conduction heat transfer equation of the perforated fin can be stated as below [13,14].

$$k \frac{d^2 T}{dx^2} = 0 \quad (3)$$

According to the Figs. 1, 2 and 3, the associated boundary conditions of the symmetry part considered for heat transfer analysis of the fin are:

- 1- At the base surface ($x = 0$)

$$T = T_b \quad (4)$$

- 2- At the perforated surfaces and the tip of the fin

$$k \cdot A_c \frac{dT}{dx} / x + h_{ps} \cdot A_{ps} (T - T_\infty) + h_{pc} \cdot A_{pc} (T - T_\infty) + h_t \cdot A_t (T_t - T_\infty) = 0 \quad (5)$$

In this study, the energy equation shown in (1) is solved numerically utilizing one dimensional finite-element technique. The corresponding variational statement as it is described in [13,14] has the following form:

$$I_n = \frac{1}{2} \int_{V_e} k \left(\frac{dT}{dx} \right)^2 dV + \frac{1}{2} \int_{A_{ps}} h_{ps} (T - T_\infty)^2 dA_{ps} + \frac{1}{2} \int_{A_{pc}} h_{pc} (T - T_\infty)^2 dA_{pc} + \int_{A_t} h_t (T_t - T_\infty) T dA_t \quad (6)$$

The variational approach in matrix notation [13] is used in formulating the algebraic equations of the problem of this perforated fin. The formulation of these equations can be found in details in [13,14]. The perforated fin elements and body discretization of the symmetry part are shown in Figs. 2 and 3. As shown in Fig. 3, surrounding each semi-perforation there are four regions labeled A, B, C and D. These regions which repeat themselves along x direction around each perforation are considered in formulating the discretization mesh and finite element equations. The regions A and D are divided into N_t elements each, while the regions B and C are divided into N_f elements each. The perforated fin length and width can be computed by the following equations:

$$L = N_x (2S_x + 2b \cdot \cos(\pi/6)) \quad (7)$$

$$W = N_y (2S_y + 2b \cdot \sin(\pi/6) + b) \quad (8)$$

To compare the perforated fin with the solid one, their dimensions (length, width, and thickness) are considered the same. The solid and perforated fin heat transfer surfaces can be computed by the following equations:

$$A_{sf} = P.L + W.t$$

$$A_{pf} = A_{sf} + N_x N_y (A_{pc} - 2A_c) \quad (9)$$

$$= A_{sf} + 6 \cdot N_x N_y (b \cdot t - b^2 \sin(\pi/3)) \quad (10)$$

The total number of elements N_e and the total number of nodes N_n are expressed as:

$$N_e = N_x (2N_f + 2N_t) \quad (11)$$

$$N_n = \text{Int}(S_x / Le) \quad (12)$$

$$N_t = \text{Int}(b \cdot \cos(\pi/6) / Le) \quad (13)$$

$$N_n = N_e + 1 \quad (14)$$

The results of this solution are the temperature distribution of the perforated fin along its length direction (along x axe). As the temperature distribution of the perforated fin along its length is obtained, then the heat dissipation rate (Q_{pf}) can be calculated by the following expression [14]:

$$Q_{pf} = 2N_y \sum_{I=1}^{N_e} \left(\frac{T_I + T_{I+1}}{2} - T_\infty \right) \left(h_{ps} \left(\frac{Pe(I) + Pe(I+1)}{2} \right) Le(I) + h_{pc} L_{pc}(I)t \right) + Q_t + Q_s \quad (15)$$

Where Q_t and Q_s are the heat dissipation from the tip and the two sides of the perforated fin, and can be calculated by the following expressions:

$$Q_t = A_t h_t (T_t - T_\infty) \quad (16)$$

$$Q_s = 2 \sum_{I=1}^{N_e} \left(\frac{T_I + T_{I+1}}{2} - T_\infty \right) (h_s \cdot Le(I) \cdot t) \quad (17)$$

The previous equations are described in full details in [14]. The theoretical maximum heat dissipation of the fin is obtained when the temperature of the whole fin body equals the fin base temperature (isothermal fin). It can be computed by the following expression:

$$Q_{pf, \max} = (A_{ps} h_{ps} + N_x N_y A_{pc} h_{pc} + A_t h_t + A_s h_s) (T_b - T_\infty) \quad (18)$$

The fin efficiency is defined as the ratio of the heat transfer from the fin in its actual temperature distribution to its maximum heat transfer. Consequently, the fin efficiency is expressed as:

$$\eta_{pf} = Q_{pf} / Q_{pf, \max} \quad (19)$$

In order to compare performance of the perforated fin with that of the solid (non-perforated) one of the same dimensions, the following equations of the solid fin consider convection heat transfer from its tip as described in [15] are used.

$$Q_{sf} = k.A.m(T_b - T_\infty) \frac{\text{Sinh}(m.L) + (h_t/(m.k)) \text{Cosh}(m.L)}{\text{Cosh}(m.L) + (h_t/(m.k)) \text{Sinh}(m.L)} \quad (20)$$

Where m is defined as

$$m = \sqrt{\frac{h \cdot P_{sf}}{k \cdot A}} \quad (21)$$

Where Q_{sf} is the heat dissipation rate of the solid fin. The ratio of the heat dissipation of the perforated fin to that of the solid one (RQF) is introduced and given by:

$$RQF = Q_{pf} / Q_{sf} \quad (22)$$

Fig. 1 shows the fin with lateral hexagonal perforations, which is investigated in this study. In particular, it is solved numerically utilizing the finite-element technique as it is described in [13]. The dissipation heat from solid or perforated fin depends on the fin temperature distribution, surface areas and heat transfer coefficients. For the solid fin, the three aspects are established. The average value of (h_{sf}) in natural convection is given by the following expression [16]:

$$h_{sf} = Nu \cdot k_{air} / L_c \quad (23)$$

where $L_c = L \cdot W / (2L + 2W)$

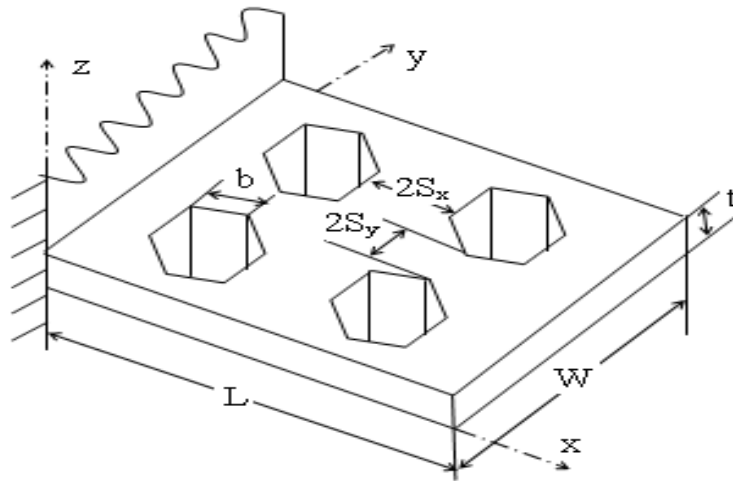


Fig. 1. The geometrical details of the perforated fin with lateral hexagonal perforations

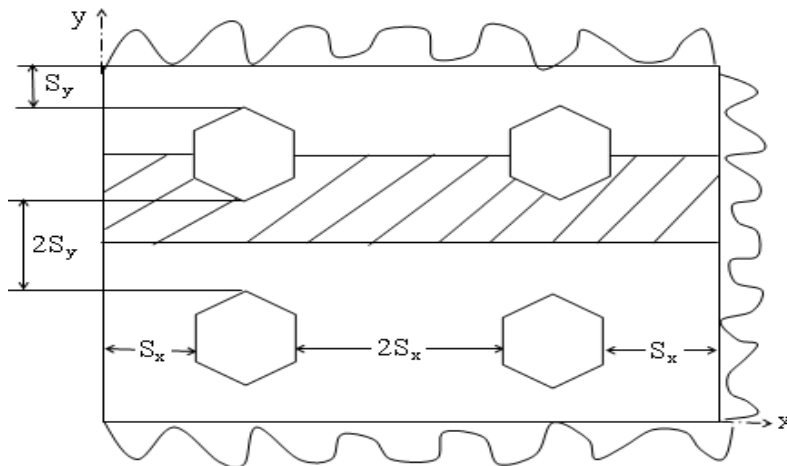


Fig. 2. The symmetrical hatched part used in the mathematical formulation of the perforated fin

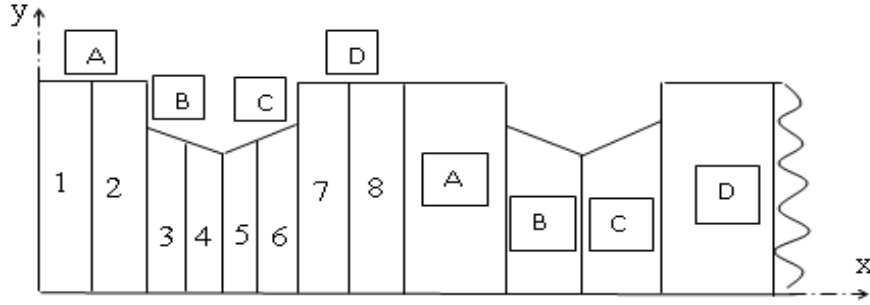


Fig. 3. Expanded symmetrical part with the four regions A, B, C and D considered in the mathematical formulation (1, 2, 3,... numbers of the linear finite elements)

The average Nusselt number, Nu , is given as [16]:

$$Nu = (Nu_u + Nu_l)/2 \tag{24}$$

$$Nu_u = \left[\left(\frac{1.4}{\ln \left(1 + \frac{1.4}{0.43 Ra^{0.25}} \right)} \right)^{10} + \left(0.14 Ra^{(1/3)} \right)^{10} \right]^{(1/10)} \tag{25}$$

$$Nu_l = \frac{0.527 Ra^{0.2}}{\left(1 + (1.9/ Pr)^{0.9} \right)^{(2/9)}} \tag{26}$$

For the perforated and non-perforated fins that are considered in this study, the fin tip is a vertical surface for which the Nusselt number is given as [16]:

$$h_{ps} = (1 + 0.75 ROA) \cdot h_{ss} \tag{29}$$

$$ROA = OA/OA_{max}$$

$$Nu_t = 0.5 \left[\left(\frac{2.8}{\ln \left(1 + \frac{2.8}{0.515 Ra^{0.25}} \right)} \right)^6 + \left(0.103 Ra^{0.333} \right)^6 \right]^{(1/6)} \tag{27}$$

$$h_t = Nu_t \cdot k_{air} / L_c \tag{28}$$

where $L_c = L \cdot t / (2L + 2t)$

The second one is the heat transfer coefficient within the perforation (h_{pc}) where its associated Nusselt number (Nu_c) is given as in the following [16]:

$$Nu_c = \left[\left(\frac{Ra_c}{15.05} \right)^{-1.5} + (0.62 Ra_c^{0.25})^{-1.5} \right]^{1/-1.5} \tag{30}$$

For the examined perforated fin there are three different heat transfer coefficients. The first one is the heat transfer coefficient of the remaining solid portion of the perforated surfaces (h_{ps}) which can be found out using the following expression [4]:

Thirdly, the heat transfer coefficient at fin tip (h_t), such that the related Nusselt number (Nu_t) of this coefficient is governed by equation (28). To evaluate the enhancement of the heat dissipation rate due to fin perforation, the performance of the perforated fin is compared with that of the equivalent solid one. This comparison can be achieved by considering the ratio of heat

dissipation of the perforated fin to that of the solid one (RQF) which can be computed by equation (22). The heat dissipation of the solid fin (Q_{sf}) is computed according to the exact solution equation (20) [15]. The weight of the perforated fin is compared with that of the non-perforated one by using the weight ratio (RWF) which is given by:

$$\begin{aligned} \text{RWF} &= W_{pf} / W_{sf} \\ &= 1 - \frac{3 N_x \cdot N_y \cdot b^2 \text{Sin}(\pi/3)}{L \cdot W} \end{aligned} \quad (31)$$

4. RESULTS AND DISCUSSION

Comparing the heat dissipation by the perforated fin with that of its solid counterpart is the best means to evaluate the improvement or worsening of heat transfer brought by introducing the perforations. Hence, It is assumed that both fins have the same dimensions (the fin length is $L= 50$ mm and its width is $W= 200$ mm), same thermal conductivity, same base and ambient temperatures (100°C and 20°C) respectively.

4.1 Temperature Distribution Patterns, $T(x)$

The temperature distribution along the perforated fin, $T_{pf}(x)$, is examined in terms of perforation parameters and fin thickness and plotted in Fig. 4. The perforation spacing $S_x = S_y = 1$ mm. The temperature distribution along the fin determines the fin performance. Higher fin temperatures means high fin efficiency and effectiveness. The higher fin temperatures exist as the fin low thermal resistance exist. As pointed out from Fig. 4, it is observable that the temperature distribution patterns show non uniform curves caused by perforations. The perforations produce a variations in cross sectional area in the direction of the fin length and then lead to a dissimilarity in the fin thermal resistance. The result of variation of cross sectional area on the fin thermal resistance due to perforation decreases as the thermal conductivity increases. This is easily can be shown from Fig. 4 as the temperature distribution curves become more uniform. To compare the temperature distribution of the perforated fin with that of the conventional (solid) one, the temperature difference distribution of the solid fin and the perforated fin ($T_{sf}(x) - T_{pf}(x)$) is plotted in Fig. 5. As shown in this figure it is obvious that the temperatures along the solid (non-perforated)

fin are always higher than those of the perforated one. This is because the thermal conduction resistance of the perforated fin is always higher than that of the corresponding non-perforated one. As the thermal conductivity increases the difference ($T_{sf}(x) - T_{pf}(x)$) decreases. (Figs. 4 and 5) show that the temperature difference (temperature drop) between the fin base and tip increases as the lateral hexagonal perforation dimension is increased. This is due to the fact that, the perforated fin thermal resistance will increase as the perforation dimension (b) is increased. According to the temperature distribution patterns, it is advised (recommended) to apply small perforation as possible. Moreover, it can be recognized from the temperature distribution that the fin temperatures increase as the fin thickness is increased. This is basically clarified by the fact that the thermal resistance of the perforated fin decreases as the fin thickness is increased. Consequently, from the viewpoint of the temperature distribution patterns, it is recommended to use large fin thicknesses as possible. This finding has a good agreement with the results that are reported by Raaid R. Jassem [8].

4.2 Ratio of Heat Dissipation Rate (RQF)

The ratio of heat dissipation rate from the perforated fin to that of the corresponding solid one (RQF) is investigated (studied) in terms of perforation dimension (b). This investigation is accomplished for many values of fin thickness ($t = 1, 2, 3, 4, 5$ mm) and for thermal conductivity of the values ($k = 100, 200, 300, 400$ W/m. $^\circ\text{C}$). Fig. 6 shows the alterations of (RQF) as a function in the perforation dimension (b) for various values of (k) ranging from 100 to 400 [W/m. $^\circ\text{C}$] and for fin thicknesses of 1, 3 and 5 mm. The alterations of (RQF) in relation with (b) at different values of (k) showed a regular trend of increasing to a maximum value then it declines. This style of variation can be explicated by taking into consideration that the combined effects of changing in fin heat transfer surface area and heat transfer coefficients due to perforations. In addition, Fig. 6 shows that (RQF) has an evident relationship with the perforation dimension (b). The hexagonal perforation dimension at which (RQF) ratio has its utmost value is referred to as the optimum (best) perforation dimension which is symbolized as (b_o). Furthermore, it can be notified that the fin thermal conductivity has a slightly impact on the optimum perforation dimension (b_o). Fig. 7 presents the variation of optimum perforation dimension (b_o) under the

range of thermal conductivity of ($k = 100$ to 400 $W/m \cdot ^\circ C$) and for different values of fin thickness ranges from 1 to 5 mm. It is clear that the fin thickness has a dominant influence on (b_o) in comparing with that of fin thermal conductivity (k). This indicates that the geometrical influence is much more than that of the thermo-physical properties of the fin material.

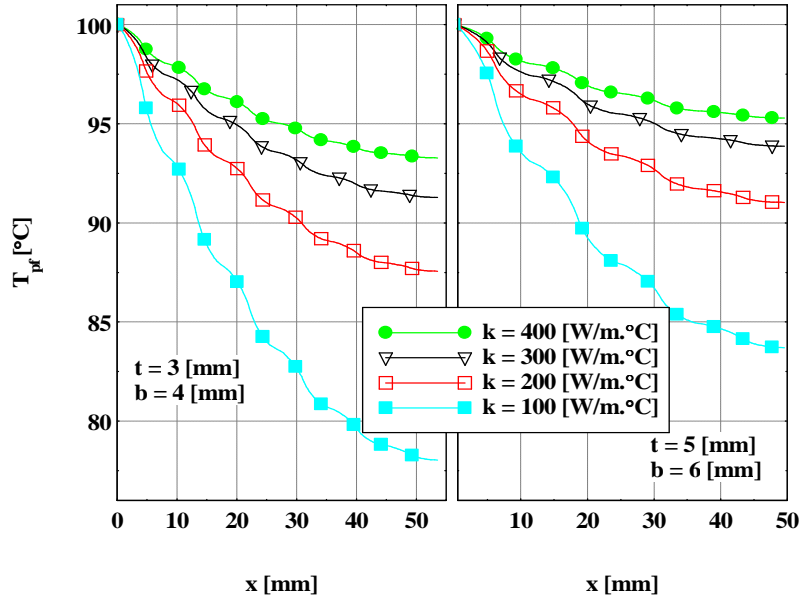


Fig. 4. Temperature distribution along the perforated fin length with variable fin thickness, perforation dimension and thermal conductivity ($S_x = S_y = 1$ mm)

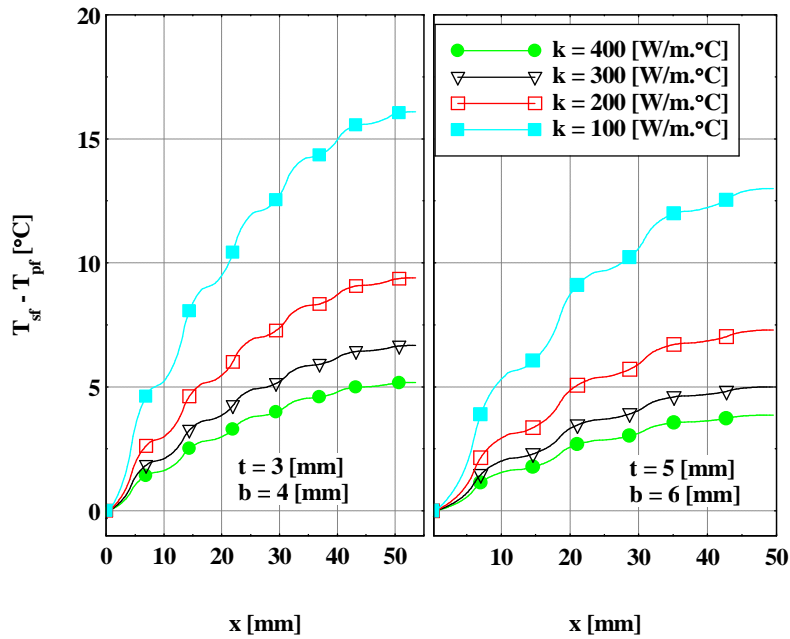


Fig. 5. Temperature difference distribution along the perforated fin length with variable fin thickness, perforation dimension and thermal conductivity ($S_x = S_y = 1$ mm)

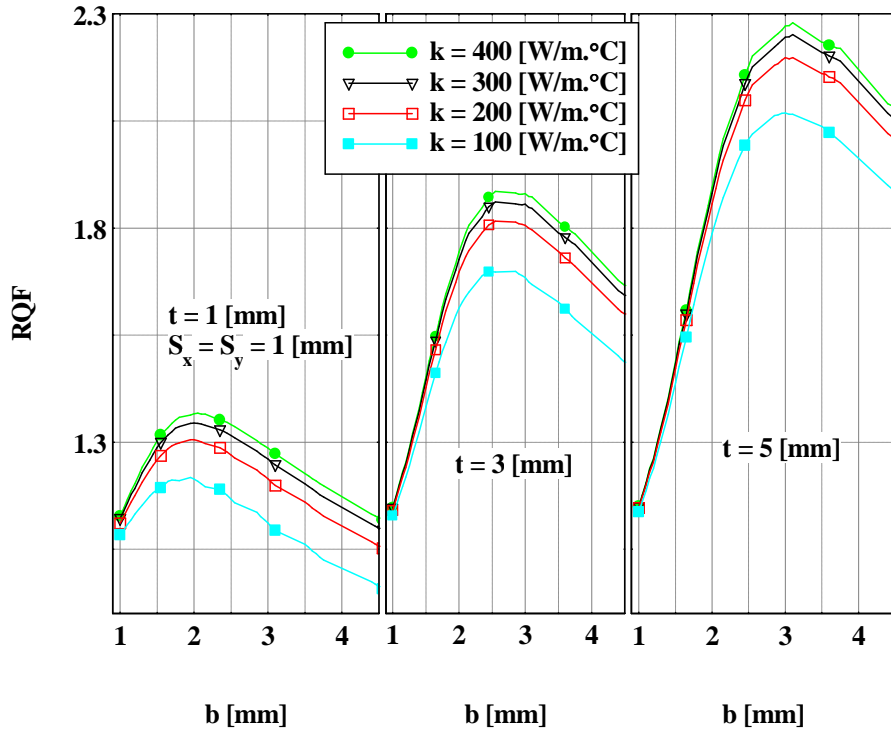


Fig. 6. The relation of ratio of heat dissipation rate (RQF) with perforation dimension under variable fin thickness and thermal conductivity

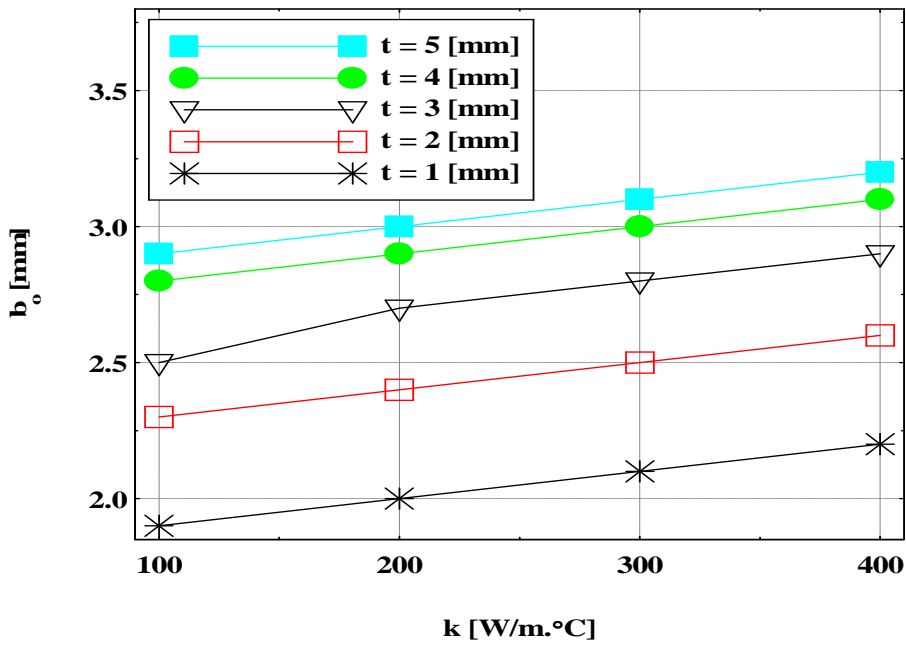


Fig. 7. Variation of the optimum perforation dimension (b_o) as a function of the fin thermal conductivity under variable fin thickness

4.3 Longitudinal Spacing (S_x) Effect on RQF

The effect of spacing (S_x) on the heat dissipation ratio (RQF) is explained in Fig. 8. This figure indicates that at any t , the (RQF) has an inversely relation with (S_x). Fundamentally, this behavior is due to the fact that increasing of (S_x) means smaller number of perforations, which means lack of the element that causes heat transfer enhancement. Consequently, it is preferable to minimize the spacing (S_x) as possible to have high rate of heat transfer augmentation.

4.4 Effect of Lateral Spacing (S_y) on RQF

The influence of lateral spacing (S_y) on the perforated fin performance is investigated. This investigation depend upon the relation between the heat dissipation ratio (RQF) with the lateral spacing (S_y). The variation of (RQF) with (S_y) is studied for various values of the fin thickness and its thermal conductivity and represented as shown in Fig. 9. It is apparent from this figure that (RQF) has a severe increase under low

values of (S_y) then tends to decline thereafter. This can be explained as, with low values of (S_y) then there is more perforations and less solid material, which increase the fin thermal resistance. This cause in a reduction in (RQF). Moreover, as the lateral spacing (S_y) increases, then there is more solid material which leads to decrease in the fin thermal resistance which cause an enlargement in (RQF). At the same time, as the lateral spacing (S_y) increases, then there is a little of perforations which leads to decrease the source of heat transfer augmentation and then to a reduction in (RQF). From the above explanation, it can be said that the inconsistent effects of fin thermal resistance and number of perforation are responsible for this style of fin thermal behavior. Fig. 9 shows that (RQF) rigorously depends on the spacing (S_y). It is obviously that there is an optimum (best) value of the spacing which is symbolized as (S_{y0}) at which (RQF) has it maximum value. The values of (S_{y0}) depend on the fin thickness and its thermal conductivity as shown in Fig. 10. This figure shows that (S_{y0}) decreases as fin thermal conductivity and its thickness increase.

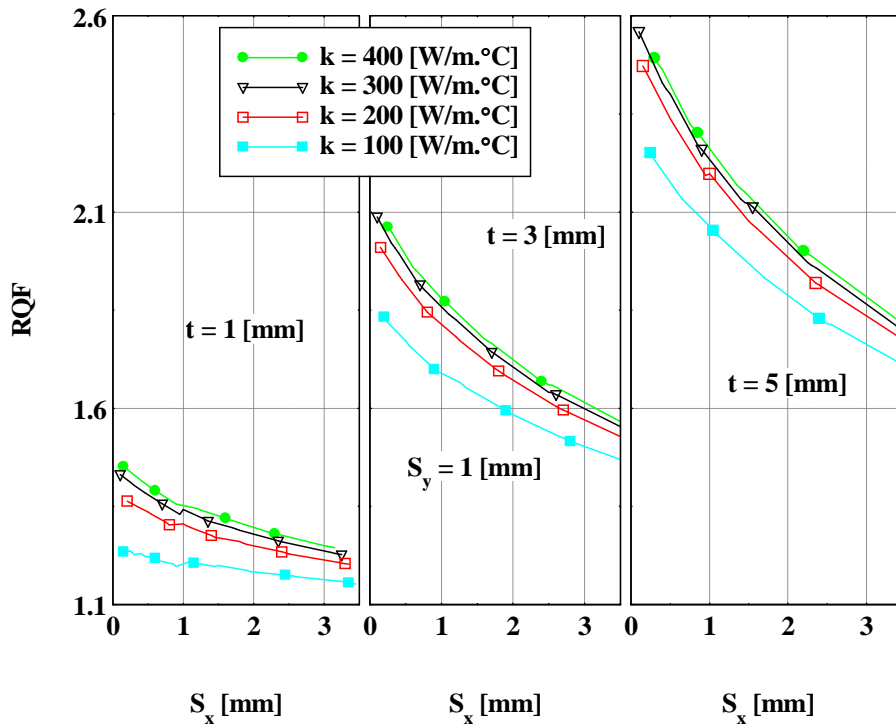


Fig. 8. Variation of ratio of heat dissipation rate (RQF) with longitudinal spacing S_x for variable fin thickness and thermal conductivity

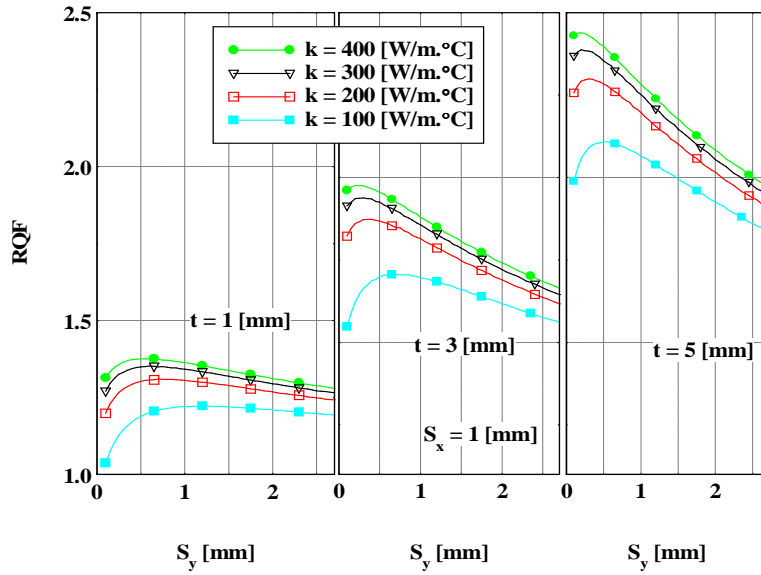


Fig. 9. Relation of ratio of heat dissipation rate (RQF) with lateral spacing (S_y) with variable fin thermal conductivity and thickness

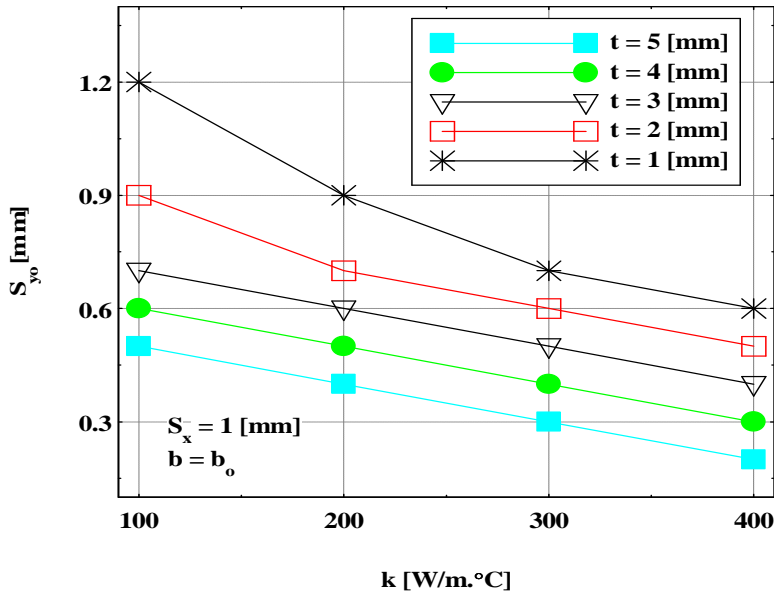


Fig. 10. Variation of optimum lateral spacing (S_{y0}) with thermal conductivity (k) for variable fin thickness

To summarize the advantages of using the perforated fin at the optimum values of perforation geometry, the heat dissipation rate (RQF) and fin weight ratio (RWF) have been investigated as a function of fin thermal conductivity for different values of fin thickness at the optimum perforation dimension (b_o) and optimum lateral spacing (S_{y0}). These relations

are plotted in Figs. 11 and 12. It can be illustrated that by means of perforations in fins it is possible to enhance heat dissipation rate and decrease the fin weight, which means lowering of the fin material expenditure. Also, the increase of fin thickness and its thermal conductivity grants a suitable opportunity for an improvement in the enhancement rate of the fin and a reduction in its

weight. Again, these findings has a good are reported by Raaid R. Jassem [8] and agreement with the experimentally results that Wadhah Hussein Abdul Razzaq Al- Doori [17].

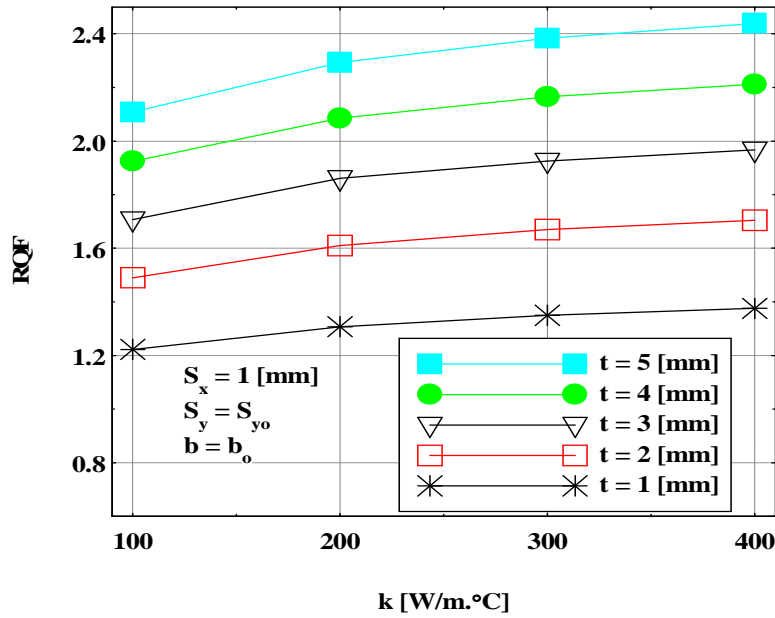


Fig. 11. Variation of ratio of heat dissipation rate (RQF) with thermal conductivity (k) at optimum perforation dimension (b_o and S_{y_o})

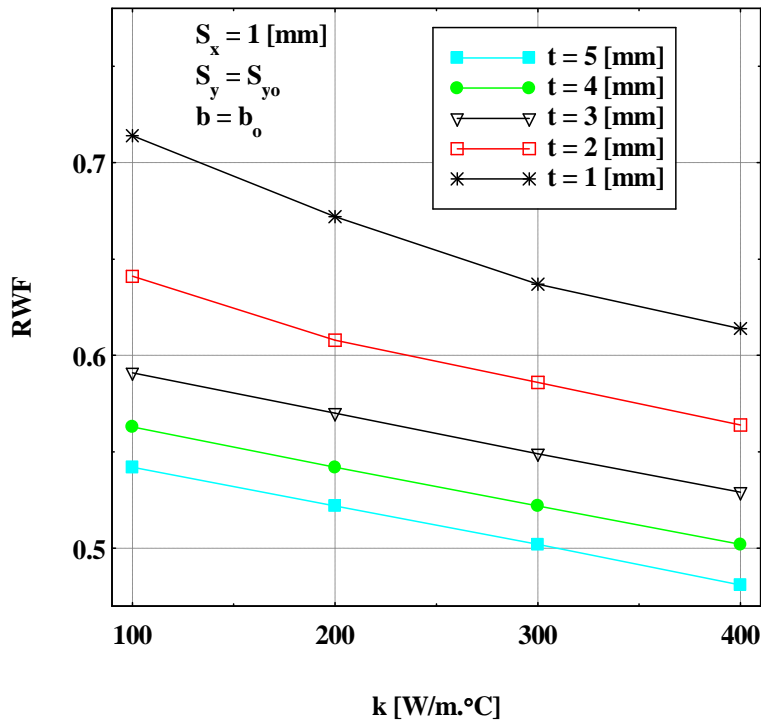


Fig. 12. Relation of fin weight ratio (RWF) with thermal conductivity (k) at optimum perforation dimension (b_o and S_{y_o})

5. CONCLUSIONS

In the light of the above analysis, it is possible to draw the following conclusions.

- 1- For certain values of lateral hexagonal perforation dimensions, the perforated fin improves heat transfer rate, such that the magnitude of augmentation is proportional to the thickness and thermal conductivity of the perforated fin.
- 2- The magnitude of the heat dissipation rate improvement for perforated fins is strongly depends on the perforation geometry and the fin thermo-physical properties.
- 3- The achievement in heat dissipation rate for the perforated fin is rigorously related to the perforation dimension and lateral spacing. This relation attains a maximum value at certain values of perforation dimension and lateral spacing. These values are called the optimum perforation dimension (b_o), and the optimum lateral spacing (S_{y_o}) respectively.
- 4- The perforation processes enhance fin heat dissipation rate and reduce its weight.

COMPETING INTERESTS

Authors have declared that no competing interests exist.

REFERENCES

1. David J. Kukulka, Kevin G. Fuller, Development of an enhanced heat transfer surface, 20th European Symposium on Computer Aided Process Engineering – ESCAPE 2010; 20, Elsevier B.V.
2. Kakac S, Bergles AE, Mayinger F. Heat exchangers, thermal-hydraulic fundamentals and design. Hemisphere Publishing Corporation; 1981.
3. Bergles AE. Techniques to enhance heat transfer, Ch. 11, In Handbook of heat transfer Applications, (Edited by Werren M. Rohsenow, James P. Hartnett, and Ejup N. Ganic), McGraw-Hill Professional; 3rd Edn, May 22; 1998.
4. Al-Essa AH, Al-Hussien FMS. The effect of orientation of square perforations on the heat transfer enhancement from a fin subjected to natural convection. Heat and Mass Transfer. 2004;40(6-7):509-515.
5. Mullisen R, Loehrke R. A study of flow mechanisms responsible for heat transfer enhancement in interrupted-plate heat exchangers. Journal of Heat Transfer-Transactions of the ASME. 1986;108(2): 377-385.
6. Kutscher CF. Heat exchange effectiveness and pressure drop for air flow through perforated plates with and without crosswind. Journal of Heat Transfer. 1994; 116(5):391-399.
7. Al-Essa AH. Enhancement of thermal performance of fins subjected to natural convection through body perforation, Ph.D. thesis, Department of Mechanical Engineering, University of Baghdad, Iraq and University of Science and Technology. Jordan; 2000.
8. Raaid R. Jassem. Effect the form of perforation on the heat transfer in the perforated fins. Academic Research International. 2013;4(3):198-207.
9. Gurav RB, Gaikwad SM, Patil JD, Ramgude AA. Finite volume analysis of convective heat transfer augmentation from horizontal rectangular fin by elliptical perforations. International Journal of Global Technology Initiatives (IJGTI). 2013;2(1):1-5.
10. Rupali V. Dhanadhya, Abhay S. Nilawar, Yogesh L. Yenarkar. Theoretical study and finite element analysis of convective heat transfer augmentation from horizontal rectangular fin with circular perforation. International Journal of Mechanical and Production (IJMPERD). 2013;3(2):187-192.
11. Razelos P, Georgiou E. Two-dimensional effects and design criteria for convective extended surfaces. Heat Transfer Engineering. 1992;13(3):38-48.
12. Aziz A, Lunadini V. Multidimensional steady conduction in convecting, radiating, and convecting-radiating fins and fin assemblies. Heat Transfer Engineering. 1995;16(3):32-64.
13. Singiresu S. Rao. The finite element method in engineering. Fourth Edition, Rao, Elsevier Science & Technology Books; 2004.
14. Abdullah H. M. Al-Essa. Heat dissipation analysis of a fin with hexagonal perforations of its one side parallel to the fin base. Yanbu Journal of Engineering and Science (YJES). 2013;7:21-30.
15. Frank P. Incropera, David P. Dewitt, Theodore L. Bergman, Adrienne S. Lavine. Fundamentals of heat and mass transfer, 6th edition. John Wiley and Sons; 2007.

16. Raithby GD, Holands KGT. Natural convection, Ch 4, In Handbook of Heat Transfer Applications (Edited by W. Rohsenow, J. Hartnett and E. Ganic), McGraw-Hill Professional; 3rd Edn, May 22; 1998.
17. Wadhah Hussein Abdul Razzaq Al- Doori, Enhancement of natural convection heat transfer from rectangular fins by circular perforations. International Journal of Automotive and Mechanical Engineering (IJAME). 2011;4:428-436.

© 2016 AlEssa and Qasem; This is an Open Access article distributed under the terms of the Creative Commons Attribution License (<http://creativecommons.org/licenses/by/4.0>), which permits unrestricted use, distribution, and reproduction in any medium, provided the original work is properly cited.

Peer-review history:
The peer review history for this paper can be accessed here:
<http://sciencedomain.org/review-history/16366>